IEEE Access
Multidisciplinary | Rapid Review | Open Access Journal

Received September 8, 2016; accepted October 14, 2016, date of publication January 10, 2017, date of current version January 27, 2017.

Digital Object Identifier 10.1109/ACCESS.2016.2637443

Characterizing Polarization-MIMO Antennas in Random-LOS Propagation Channels

AIDIN RAZAVI, ANDRÉS ALAYÓN GLAZUNOV, (Senior Member, IEEE), PER-SIMON KILDAL, (Fellow, IEEE), AND JIAN YANG, (Senior Member, IEEE)
Department of Signals and Systems, Chalmers University of Technology, 412 96 Gothenburg, Sweden

Corresponding author: A. Razavi (aidin.razavi@chalmers.se)

This work has been supported by two projects from Sweden's innovation agency VINNOVA, one within the VINN Excellence Center Chase at Chalmers and another via the program Innovative ICT 2013, and by internal support from Chalmers.

ABSTRACT In the 5G system, we foresee the use of LOS-dominated mm-wave radio links to moving users being subject to slow fading resulting from the users' random locations and orientations. We refer to this as a random-LOS channel. MIMO processing algorithms will be used in 5G to improve performance in slow fading, similar to how they are used in Rayleigh fading. To this end, we study the probability of detection in the random-LOS channel when there are dual-polarized antennas on both sides of the link. We introduce two polarization deficiencies: the polarization non-orthogonality and the amplitude imbalance between the ports of a two-port antenna. The MIMO efficiency is evaluated as a function of these deficiencies. In the analysis, we consider the MRC algorithm for one bitstream, and the ZF and SVD algorithms for two bitstreams. We also present two analytical formulas for the MIMO efficiency that can be used to determine performance. We use the formulas on two ideally orthogonal dipoles, and show by means of coverage plots how much the 1- and 2-bitstream performances degrade due to the polarization deficiencies in off-boresight directions.

INDEX TERMS Antenna theory, line-of-sight, polarization-MIMO, antenna measurements.

I. INTRODUCTION

Polarization multiplexing is used in traditional fixed Line-Of-Sight (LOS) communication systems where the antennas on the two sides of the radio link are fixed and aligned with each other, such as terrestrial and satellite communications links [1]. The intention of polarization multiplexing is to transmit two different bitstreams over the link at the same time by using two orthogonal polarizations. Ideally, there is no need for post-processing of the received signals in order to separate the two bitstreams, because the two polarizations of both the transmitting and receiving antennas are aligned with each other already during their installation. The present paper addresses the problem when the polarizations on the two sides are *not* aligned in a LOS system due to, e.g., a randomness during installation, or because one side (the user side) is mobile [2].

In scattering environments it is not possible to align the polarizations on the transmitting and receiving sides during installation, due to the *multipath*. Therefore, the Multiple-Input Multiple-Output (MIMO) technology was introduced to solve the problems of random polarization, and at the same time the Rayleigh fading, by using an array of separate antenna elements on at least one side of the link. The elements should have orthogonal polarizations, or spacings not smaller than half-wavelength [3]. In multipath channels, it is possible to transmit more than two bitstreams if there are more than two elements on each side of the link. The present paper uses MIMO technology in LOS even though there is no multipath. Spatial multiplexing by MIMO technology was previously attempted in LOS radio links and satellite systems with given polarization, but unfortunately the antenna element separations had to be many times larger than half-wavelength in LOS [4, Sec. 3.2] and thereby became impractical. However, in the LOS environments where the polarization is completely arbitrary, the use of MIMO technology enhances the system performance. This arbitrariness appears in LOS systems when the antenna on one side of the link is subject to user randomness. The current paper's focus is on the study of this case.

Both anechoic chambers (with absorbers on the walls) and reverberation chambers (with reflecting walls) [5], [6] can be used for Over The Air (OTA) testing of wireless devices for 3G and 4G wireless systems. The reverberation chamber emulates a Rich Isotropic Multipath (RIMP) environment [6],

representing a good model for environments with a lot of multipath due to scattering, such as indoor and urban environments. The anechoic chamber, representing a pure LOS environment, is a traditional test environment for measuring the performance of antennas for fixed installations.

The 5G wireless system is expected to include communications to the users via millimeter wave links, and at millimeter wave frequencies the multipath is less pronounced and the LOS gradually takes over the dominant role. However, the user side of a 5G wireless communication link will suffer from slow fading due to the random location and orientation of the users and the way they use their terminals [7]. Therefore, MIMO antenna systems must be designed to account for such slow fading of the LOS contribution. The term Random Line-Of-Sight (Random-LOS) has been introduced to describe this new representative OTA test scenario [8], [9], and to denote the channel model.

The RIMP and Random-LOS are opposite so-called edge environments (and of course also the corresponding channel models). It is well known that antenna efficiency and coupling are relevant antenna parameters in RIMP. A similar understanding for Random-LOS has been lacking until now. This understanding is crucial in order to develop appropriate OTA test methods and characterizations for the 5G system. Furthermore, using polarization diversity can improve the system performance when the polarization is arbitrary in LOS [10], [11]. However, in Random-LOS not only the polarization of the incoming wave is random, but also its Angle-of-Arrival (AoA). It is known that the two ports of a dual-polarized antenna does not provide orthogonal and equal amplitude far-fields at all directions. However, there does not exist a set of parameters that fully characterize polarization MIMO in Random-LOS with focus on the antenna performance.

The current paper therefore aims to provide new insights into the requirements on polarization-MIMO antennas in the Random-LOS (random polarization and random AoA) channels. The contributions of the paper are summarized as follows:

- We propose two new figures of merit to characterize antennas and their impact on the polarization-MIMO system performance due to polarization deficiencies, i.e., the *polarization non-orthogonality* and *amplitude imbalance* between the two ports of the antenna on one side of the link. It is worthwhile to note that these deficiencies may still be present even if the ports themselves are orthogonal, i.e., uncoupled. The introduced deficiencies of general antennas in a Random-LOS environment have been much less understood and have not been investigated by others.
- We show, based on examples, how these deficiencies can easily represent the spatial or rather angular performance of the antennas. While the focus of this paper has been on hemispherical coverage, it is straightforward to expand the concept to the complete spherical coverage or to any other specific solid angle. The analysis is carried out first time by applying the two introduced deficiencies.
- We also present two new analytical formulas for the polarization-MIMO efficiency that can be used to determine performance independently of the algorithm used at the receiver.
- Finally, we show, based on the MIMO efficiency characterization of various algorithms, the importance of the Random-LOS environment to analyze the performance of the antennas. We provide numerical values of the required transmit power to achieve 90% or 95% Probability of Detection (PoD), i.e., normalized throughput, of 1- or 2-bitstreams with polarization-MIMO in Random-LOS.

To this end, we will first introduce the two polarization deficiencies and illustrate how to characterize polarization randomness in terms of a degradation of the PoD for both the 1- and 2-bitstream cases, i.e., for the SIMO and MIMO cases, respectively. These degradations can be referred to as MIMO efficiencies, and we plot them versus the two polarization deficiencies. At the end, we show how to present bitstream coverage plots and PoDs for complete antenna far-field, using orthogonal dipoles on the receiving side as an example. The current study has been based on own implementations of Random-LOS MIMO in MATLAB using the commonly known MIMO algorithms MRC (Maximum Ratio Combining), ZF (Zero Forcing), and SVD (Singular Value Decomposition), and the ViRMlab simulation tool described in [12] that has been extended with the 2-bitstream MIMO algorithms.

II. ANTENNA POLARIZATION DEFICIENCIES

Generally, the two ports of a dual-polarized antenna have orthogonal far-field functions only in one main direction. If the antenna has two symmetry planes, the far-fields of the two ports will also be orthogonal in the symmetry planes, but they may not be amplitude-balanced there. The reason is that the E- and H-plane patterns of antennas often are different. Furthermore, between the symmetry planes there can be significant cross-polar field levels (see, e.g., the BOR_1 antenna relations in [13, Sec. 2.4.2]). These deficiencies will affect the system performance in a Random-LOS environment, but in a different way than in a fixed LOS-dominated polarization multiplexing system.

It is well known that it is possible to combine the channels on the ports of a dual-polarized antenna in such a way that the resulting polarization is aligned to any polarization of the incident wave. In a MIMO system this is automatically achieved by using the MRC algorithm [13, Sec. 3.10]. Therefore, the envelope of the combined signal will in this case be constant, i.e., independent of the orientation of the relative polarization of the antenna and the polarization of the incident wave. However, this will not happen for those AoAs where the far-fields of the two antenna ports are non-orthogonal or amplitude-unbalanced. Whereas small orthogonal antennas very often have far-fields that are orthogonal and balanced

only in one specific main direction. This is in particular the case for orthogonal dipole and patch antennas.

Let us assume that the far-field functions[1] of the two receiving antennas are defined as $\boldsymbol{G}_1(\theta,\phi)$ and $\boldsymbol{G}_2(\theta,\phi)$ at any direction (θ,ϕ) in space. Then, we can define the *amplitude imbalance* as

$$I_{\mathrm{a}}(\theta,\phi) = \frac{\max\{|\boldsymbol{G}_1|,|\boldsymbol{G}_2|\}}{\min\{|\boldsymbol{G}_1|,|\boldsymbol{G}_2|\}}, \tag{1}$$

which is the ratio of the amplitudes of the two far-field functions, and $1 \le I_{\mathrm{a}}(\theta,\phi)$.

Moreover, we define the *polarization non-orthogonality* as

$$I_{\mathrm{p}}(\theta,\phi) = \frac{|\boldsymbol{G}_1 \cdot \boldsymbol{G}_2^*|}{|\boldsymbol{G}_1|\,|\boldsymbol{G}_2|}. \tag{2}$$

The far-field functions are desired to be as close to orthogonal as possible, hence when $\boldsymbol{G}_1$ and $\boldsymbol{G}_2$ are orthogonal, we have $I_{\mathrm{p}} = 0$. I_{p} reaches its maximum when the two far-field function vectors are parallel, and in general, $0 \le I_{\mathrm{p}}(\theta,\phi) \le 1$.

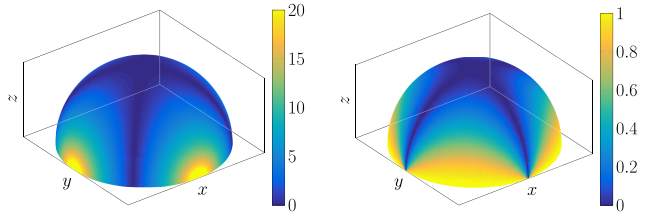

(a) (b)

FIGURE 1. (a) I_{a}, amplitude imbalance in dB, and (b) I_{p}, polarization non-orthogonality, of two orthogonal half-wave dipoles oriented along the x- and y-axes, respectively.

A. EXAMPLE: TWO ORTHOGONAL DIPOLES

The polarization non-orthogonality and amplitude imbalance may both be pronounced (i.e., $I_{\mathrm{a}} \gg 1$, and I_{p} closer to 1 rather than 0) at most AoAs, even if the antenna elements (ports) themselves are orthogonal, i.e., uncoupled. We will illustrate this by an example. We consider two co-located orthogonally polarized half-wave dipoles, located at the origin of the coordinate system. The dipoles are assumed to be x- and y-polarized, respectively. Knowing the far-field function of the half-wave dipole, I_{a} and I_{p} can be determined for every θ and ϕ angle. Fig. 1 shows the spatial distribution of I_{a} in dB and I_{p} in this combination, in the half-space above the xy-plane. We observe that except for the boresight direction, the orthogonal receiving antenna ports are not providing orthogonal polarizations with equal amplitude. Though two half-wave dipoles are used for this example, similar imbalances may also appear away from broadside for other orthogonal antennas. Actually, it is known that rotationally symmetric antenna structures providing pencil beams will generally have cross-polar sidelobes in the 45° planes. This is shown in, e.g., [13, Sec. 2.4.2] about the so-called BOR_1 antennas. Exceptions are the incremental Huygens source [13, Sec. 4.4.3], and corrugated horn antennas [13, Sec. 8.8] which both have very low (ideally zero) cross-polar level in all azimuthal planes.

[1]It should be noted that we use bold vector notation for the far-field functions $\boldsymbol{G}(\theta,\phi)$, which shall not be confused with gain $G(\theta,\phi)$. We follow the notation introduced in [13].

III. DIGITAL THRESHOLD RECEIVER MODEL

In a communication system, Probability of Detection (PoD) is the probability of receiving a bitstream at the receiver, with no errors. In order to determine the PoD, we use the ideal digital threshold receiver model [14]. This model was originally introduced to model the throughput of digital communication systems in the RIMP environment [15]. The ideal threshold receiver model is based on the simple fact that in modern digital communication systems, the error rate (i.e., the failure to detect a bitstream) will abruptly change from 100% (all errors) to 0% (no error) in a stationary AWGN channel, due to the use of advanced error correction schemes. This means that as soon as the received signal-to-noise ratio (SNR) or the received power reaches a certain threshold level, the error rate will drop to 0%. The threshold level is determined by the receiver's design and the wireless system specifications; and can be determined with conductive measurements if a measurement port is available at the device.

According to the ideal threshold receiver model, the PoD can be written as [14]:

$$\mathsf{PoD}(P/P_{\mathrm{th}}) = \frac{\mathsf{TPUT}(P/P_{\mathrm{th}})}{\mathsf{TPUT}_{\max}} = 1 - \mathsf{CDF}(P_{\mathrm{th}}/P), \tag{3}$$

where P_{th} is the threshold level of the receiver, P is a reference value proportional to the transmitted power, PoD is the Probability of Detection function, TPUT is the average throughput, and CDF is the Cumulative Distribution Function (CDF) of the received fading power P_{rec} normalized to the reference (P_{rec}/P). In the case when the received power does not undergo fading, the PoD is a step function, where the transition from $\mathsf{PoD}=0$ to $\mathsf{PoD}=1$ occurs at the threshold level, i.e., for $P = P_{\mathrm{th}}$. The power values relative to P_{th} are shown in dBt, which is the dB value relative to the threshold level of the receiver itself.

In the RIMP case the received power undergoes Rayleigh fading. Hence, the CDF in (3) is described by the Rayleigh probability distribution function. The average of the Rayleigh distribution is then used as the reference power in RIMP, i.e., $P = P_{\mathrm{av}}$. In the Random-LOS case where we deal with polarization randomness, the maximum received power is used as the reference value, i.e., $P = P_{\max}$. The maximum received power occurs when the polarization of the receiver is aligned with that of the incident wave.

To illustrate the digital threshold receiver model and PoD for Random-LOS, let's first consider the simple case of one transmitting and one receiving antenna, i.e., a Single-Input Single-Output (SISO) system. Both antennas are assumed to be linearly polarized, but have arbitrary polarization with respect to each other. The relative orientation of the polarization of the two antennas is given by a random angle with uniform distribution between 0 and 2π radians. Then, the

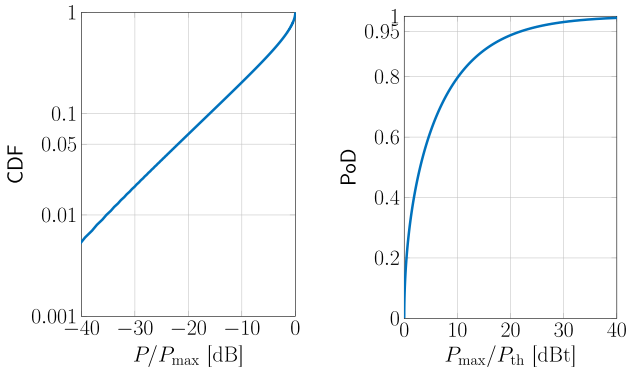

FIGURE 2. Illustration of ideal threshold receiver model for a simple LOS link with uniformly random polarization mismatch (a) the CDF, and (b) the PoD.

probability distribution of the normalized received power $P/P_{\max}$ becomes that of a squared cosine function. The corresponding CDF is plotted in Fig. 2(a). This CDF plot shows that, e.g., for 5% of the states, the received power is at least 22 dB below $P_{\max}$. This means that for the remaining 95% of cases the received power is within 22 dB of the maximum received power, i.e., the polarization-aligned case. Hence, if the maximum available power is 22 dB above the threshold level of the receiver, there is 95% probability that the received power will still be above the threshold level, in the presence of polarization mismatch. When at a given fading state the received power is higher than the threshold level, the bitstream can be detected with no error. So, in our example, maximum power being 22 dB above the threshold level means that the PoD will be 95%. This is also shown when the ideal threshold receiver model as described by (3) is used to obtain the PoD. The PoD of the SISO system in Random-LOS is plotted in Fig. 2(b). This figure shows that in order to maintain an error-free link for 95% of the time, the maximum received power needs to be at least 22 dB higher than P_{th}, i.e., 22 dBt.

IV. MIMO EFFICIENCY

The power required to achieve the 95% PoD level is often used as a metric for the system performance [15], [16]. This value represents the power that is required at the transmitter in order for 95% of the data packets to be detected at the receiving side for a fixed coding and modulation scheme. MIMO efficiency is defined by the $P_{\max}/P_{\text{th}}$ degradation compared to an ideal antenna, in the presence of polarization deficiencies. The ideal antenna is naturally the case where I_{a} in dB and I_{p} are both equal to zero, i.e., orthogonal and equal-amplitude far-fields on the two ports. Hence, MIMO efficiency can be expressed as:

$$\eta_{\text{MIMO}} = \frac{\text{PoD}_0^{-1}(0.95)}{\text{PoD}^{-1}(0.95)}, \tag{4}$$

where PoD^{-1} is the inverse function of PoD, and PoD_0 represents the PoD of the ideal case with no deficiencies as defined in section II. Hereafter, we use the MIMO efficiency to investigate the effect of the polarization deficiencies on the MIMO system performance, for both 1- and 2-bitstream cases. It is clear that a higher $P_{\max}/P_{\text{th}}$ value means that higher transmitted power is required to maintain the 95% PoD level, thus a poorer system performance. This will in turn show itself in decreased MIMO efficiency. The MIMO efficiency can then be calculated for any given antenna at any AoA. We can even readily extend the definition to a given range of AoAs, i.e., a given bitstream coverage, to get the MIMO efficiency as a function of AoA [17]. We use this definition later in Fig. 7 and Fig. 8 to plot the bitstream coverage for dipole antennas using different MIMO algorithms. When we evaluate the MIMO efficiency for a 2×1 MIMO system, it corresponds in reality to a SIMO efficiency. We herein use MIMO as a general term covering also the SIMO and the MISO cases.

A. 1-BITSTREAM CASE

We will first investigate the 1-bitstream case in Random-LOS, by using the MRC algorithm to determine the CDF and PoD when the polarization is random for a given AoA. In the main broadside direction the receiving antenna ports in the example of dipole antennas (described above) have orthogonal far-field functions with equal amplitude. The MRC algorithm will always align the polarization of the receiving side with that of the transmitting side. Therefore, we use herein this polarization-aligned case as a reference, when determining the MIMO efficiency.

For the 1-bitstream case with the MRC algorithm, it is also possible to define the efficiency based on the degradation in the diversity gain at 5% level. However, it can be shown that such definition will yield the exact same efficiency values as the definition based on the PoD. Hence, to avoid repetition, we do not present efficiencies based on diversity gain; and the same MIMO efficiency is used for both the 1-bitstream and the 2-bitstream cases. It should be mentioned that the diversity gain in RIMP is often defined at the 1% CDF level [18], [19]. Instead, here we choose in Random-LOS a definition at the 5% CDF level (corresponding to the 95% PoD level) because in practical situations this can be determined much more accurately than at the 99% PoD level. In addition, 95% is often used as the reference for relative throughput performance, see, e.g., [15].

B. 2-BITSTREAM CASE

For the 2-bitstream systems, it's assumed that two transmitting and two receiving antennas are employed to transmit two separate bitstreams. Since the polarizations of the two ends of the link are not necessarily aligned in Random-LOS, MIMO algorithms are needed to separate the two bitstreams at the receiver. Here, we use Zero Forcing (ZF) and Singular Value Decomposition (SVD) algorithms and compare the performance of both algorithms in the presence of polarization deficiencies as defined in section I.

For the two bitstreams case, the above definition of degradations at the 95% PoD level will correspond to the MIMO

efficiencies defined in [16] and [20] for RIMP environments. The difference between RIMP and Random-LOS is the choice of the reference level. While the maximum i.i.d. level is used in RIMP as the reference, the orthogonal dual-polarized equal-amplitude antenna with 100% radiation efficiency is used as the reference in Random-LOS.

In 2-bitstream systems, each of the separate bitstreams has its own PoD curve. The PoDs of the two bitstreams are not necessarily equal. The MIMO efficiency of a 2-bitstream system is defined based on the worse performing bitstream, i.e., the one with lower received power. The reason for this choice is that it is the worse channel that limits the system's performance in practice.

V. 1-BITSTREAM 2 × 1 DIVERSITY (SIMO) SYSTEMS

We start by studying how the MIMO efficiency of a 2 × 1 diversity system, i.e., a SIMO system, degrades with polarization non-orthogonality and amplitude imbalance at individual AoAs. Since the transmitting and receiving antennas are typically located in the far-field region, we can assume an incoming plane wave with random linear or circular polarization $\boldsymbol{E}_\mathrm{i}$. We choose linearly polarized receiving antennas since this is what is commonly used in practical wireless communication systems. We model them by their corresponding far-field functions, $\boldsymbol{G}_1$ and $\boldsymbol{G}_2$. Depending on the AoA of the incoming plane wave, $\boldsymbol{G}_1$ and $\boldsymbol{G}_2$ make an angle α with each other between 0 and π radians. Also, the amplitudes of $\boldsymbol{G}_1$ and $\boldsymbol{G}_2$ are dependent on the AoA. The amplitudes and the angle α, determine the deficiencies as defined in (1) and (2), respectively. In the case of a linearly polarized incoming wave (LP), the $\boldsymbol{E}_\mathrm{i}$ and $\boldsymbol{G}_1$ vectors make a random angle β with each other, corresponding to the random polarization of the plane wave as shown in Fig. 3.

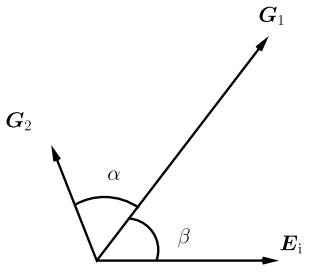

FIGURE 3. Two receiving antennas with polarization non-orthogonality and amplitude imbalance in a 2 × 1 diversity system at an arbitrary AoA. I_p and I_a are dependent on AoA and are obtained from G_1 and G_2.

The curves in Fig. 4(a) show the MIMO efficiency degradations due to amplitude imbalance. Here, we have assumed that the two far-field patterns are orthogonal and I_a varies between 0 and 20 dB, while the combined MRC gain of the two antennas is constant, i.e.,

$$|\boldsymbol{G}_1|^2 + |\boldsymbol{G}_2|^2 = constant. \tag{5}$$

As can be seen from Fig. 4(a), an amplitude imbalance of 10 dB between the two receiving antennas requires almost

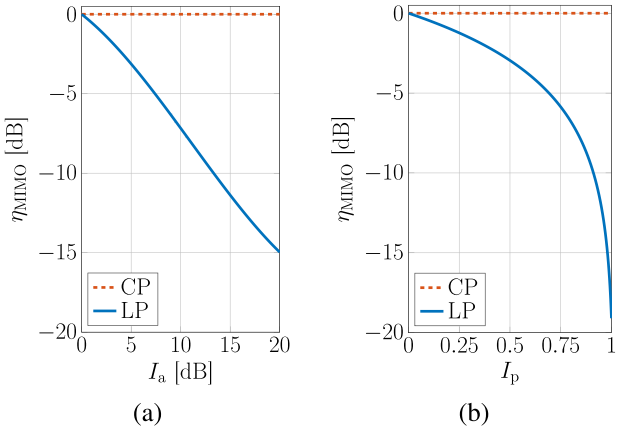

FIGURE 4. The MIMO efficiency vs. (a) the amplitude imbalance, and (b) the polarization non-orthogonality. 1-bitstream in 2 × 1 diversity system.

7 dB more power in order to maintain 95% PoD, while an amplitude imbalance of 20 dB will reduce the MIMO efficiency with almost 15 dB. For circular polarization (CP), it can be observed that the MIMO efficiency is independent of the deficiency. It should be noted that if the MIMO efficiency was defined based on the diversity gain, it could be misleading if the diversity gain was measured relative to the antenna port with the best signal, because changes in one power level will also affect the other one according to (5). Therefore, it's more informative if the diversity gain is evaluated relative to the mean of the powers at both antenna ports. By choosing this mean value as the reference, the diversity gain's degradation at 5% due to the amplitude imbalance will be identical to that of the 95% PoD level. Since the diversity gain plots convey exactly the same information as the PoD plots, we have not included them in the current paper.

Similar curves can be evaluated for the non-orthogonality I_p as shown in Fig. 4(b). These are obtained by assuming that the two antenna far-fields have equal amplitudes at a given AoA. If $\boldsymbol{G}_1$ and $\boldsymbol{G}_2$ are orthogonal, the MRC can recover the received signal regardless of the polarization of the incident field [13, Sec. 3.10]. But if the far-fields are not orthogonal, the MIMO efficiency will be reduced. The MIMO efficiency vs. polarization non-orthogonality is plotted in Fig. 4(b). This figure shows that the communication link performs best when $\boldsymbol{G}_1$ and $\boldsymbol{G}_2$ are orthogonal ($I_\mathrm{p} = 0$), whereas it degrades with the increase in the polarization non-orthogonality. The worst situation is when $\boldsymbol{G}_1$ and $\boldsymbol{G}_2$ are parallel ($I_\mathrm{p} = 1$).

As shown in Fig. 4(b), if the incident wave has circular polarization, the MIMO efficiency is independent of I_p. In this case, each of the two antennas will receive half of the radiated power, and the MRC combined power will add them in the optimal way regardless of I_p. In the case of linear polarization, it can be observed that 3 dB more power is required to achieve 95% PoD when $I_\mathrm{p} = 0.5$, compared to the case of $I_\mathrm{p} = 0$, i.e., for orthogonal far-field functions. Whereas, when the two antenna far-field patterns are parallel ($I_\mathrm{p} = 1$), 19 dB more power is required to achieve 95% PoD level. This is much more than in RIMP environments. Again,

the degradation in the diversity gain at 5% CDF is not plotted since it is identical to the MIMO efficiency defined at the 95% PoD level.

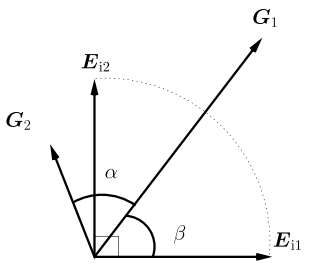

FIGURE 5. Two receiving antennas with polarization non-orthogonality and amplitude imbalance in a 2 × 2 MIMO system at an arbitrary AoA. I_p and I_a are dependent on AoA and are obtained from G_1 and G_2.

VI. 2-BITSTREAM 2 × 2 MIMO SYSTEMS

For a 2 × 2 MIMO system, the incoming signals are modeled either as two orthogonal linearly polarized plane waves with random polarization (as shown in Fig. 5), or as two circularly polarized waves $\boldsymbol{E}_{i1}$ and $\boldsymbol{E}_{i2}$ (left-hand and right-hand circular, respectively). The incoming plane waves are orthogonally polarized with respect to each other, but have an arbitrary polarization relative to the receiving antenna. In order to maintain the same transmitted power as for the diversity system, each of $\boldsymbol{E}_{i1}$ and $\boldsymbol{E}_{i2}$ contains 3dB less power than the $\boldsymbol{E}_i$ of the 2 × 1 diversity system, as it is common in all MIMO system analysis to fix the total radiated power. The receiving antennas are again modeled by their corresponding far-field vectors $\boldsymbol{G}_1$ and $\boldsymbol{G}_2$. Depending on the AoA of the incoming plane wave, $\boldsymbol{G}_1$ and $\boldsymbol{G}_2$ make an angle α between 0 and π radians. In the case of linear polarization, the vector directions of $\boldsymbol{E}_{i1}$ and $\boldsymbol{G}_1$ make a random angle β, corresponding to a random polarization of the incoming plane waves. The amplitude imbalance and polarization non-orthogonality are again defined by (1) and (2), respectively and are dependent on the AoA. In order to separate the two bitstreams contained in the two plane waves, the ZF and SVD algorithms are employed and their performance is compared. For the SVD algorithm, two different power allocation schemes are compared. These two are the equal power allocation and the inverse power allocation [21]. With the inverse power allocation, higher power is allocated to the bitstream that has the worse eigen-channel, based on the CSI information at the transmitter side. As mentioned earlier, for the MIMO efficiency of 2-bitstream cases, we use the worse performing bitstream, because in practice the worse channel is the one which limits the system's performance.

Assuming orthogonal receiving far-field patterns ($I_p = 0$), the effect of the amplitude imbalance on the MIMO system performance can be studied. The MIMO efficiency is plotted vs. I_a in Fig. 6(a). The graph shows curves for ZF and SVD algorithms with both linear and circular polarizations on the transmitter side. In the case of SVD both equal and inverse power allocation schemes are investigated. We can observe in Fig. 6 that different algorithms and polarizations

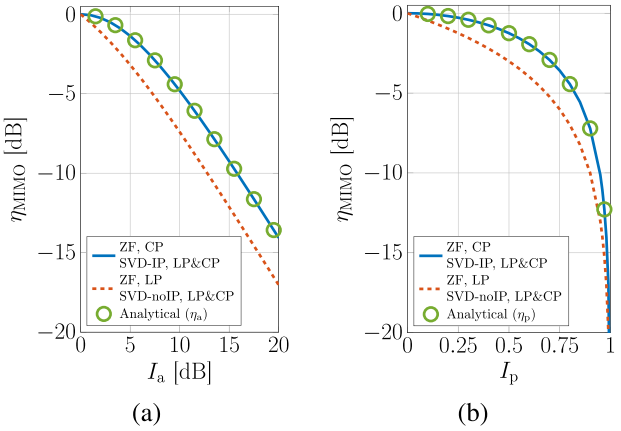

FIGURE 6. The MIMO efficiency vs. (a) the amplitude imbalance, and (b) the polarization non-orthogonality. 2-bitstream in 2 × 2 MIMO system. IP refers to inverse power allocation. LP and CP refer to linear or circular polarization of the incident wave, respectively.

can be grouped in two distinct groups, based on their corresponding MIMO efficiency degradations due to the presence of the polarization deficiencies. One group contains the ZF algorithm with circular polarization and inverse power SVD with both linear and circular polarizations. Whereas, the second group contains ZF with linear polarization and SVD with equal power allocation, regardless of polarization. As can be seen from Fig. 6(a), the second group of systems' MIMO efficiency decreases slightly more due to the amplitude imbalance than a 1-bitstream 2 × 1 system. Additionally, we observe in Fig. 6(a) that the use of circular polarization is advantageous only if the ZF algorithm is used. Still the advantage of using circular polarization at the transmitter side is much smaller in the 2 × 2 2-bitstream system than the 1-bitstream system.

Fig. 6(b) shows the MIMO efficiency vs. I_p, when assuming no amplitude imbalance ($I_a = 0$ dB). Again we see that the same above groups can be formed. We see that the effect of the polarization non-orthogonality on the MIMO efficiency of the second group is similar to that of the 1-bitstream system. Whereas the first group's MIMO efficiency degrades slightly less in the presence of the non-orthogonality. Again it is observed that the advantage of using circular polarization at the transmitter side is smaller in the 2 × 2 system than in a 1-bitstream system. Furthermore, we observe that in the extreme case of $I_p = 1$ (i.e., parallel far-field vectors), infinite power is required to maintain the 95% PoD. This is expected, since we cannot create two bitstreams in a LOS environment without using polarization multiplexing.

It is possible to derive analytical formulas for the MIMO efficiencies in Random-LOS, in the same way as it was done in [20] for 2-bitstream in RIMP. The MIMO efficiency in Random-LOS due to non-orthogonality is very close to the orthogonality factor in the 45° plane, i.e.,

$$\eta_p = 1 - I_p^2. \tag{6}$$

The MIMO efficiency in symmetry planes is proportional to the harmonic mean of the powers of the two far-field

functions in the symmetry planes [20], normalized to the mean of the powers of the two far-field functions $((|\boldsymbol{G}_1|^2 + |\boldsymbol{G}_2|^2)/2)$, i.e.,

$$\eta_{\mathrm{a}} = \frac{2|\boldsymbol{G}_1|^2|\boldsymbol{G}_2|^2}{|\boldsymbol{G}_1|^2 + |\boldsymbol{G}_2|^2} \cdot \frac{2}{|\boldsymbol{G}_1|^2 + |\boldsymbol{G}_2|^2} = \frac{4I_{\mathrm{a}}^2}{(I_{\mathrm{a}}^2 + 1)^2}. \quad (7)$$

The symmetry planes correspond to the planes where the two ports have orthogonal polarizations, but they have amplitude imbalance. The aforementioned analytical efficiencies are also plotted in Fig. 6. We see that the analytical efficiencies are in very good agreement with the MIMO efficiency when the ZF algorithm is used with circular polarization or when inverse power allocation is used with the SVD algorithm regardless of polarization.

A. EXAMPLE: TWO ORTHOGONAL DIPOLES

The MIMO efficiency for given antennas can be computed and plotted over a range of directions. This will result in bitstream coverage plots which show the performance of the MIMO system over the expected coverage area of the antennas. For the bitstream coverage plots in Random-LOS, the PoD for each individual single AoA is calculated assuming a random polarization for the incident wave. Then, we determine the MIMO efficiency by comparing each AoA to the AoA where we have the best performance, i.e., the boresight in the case of the two dipoles.

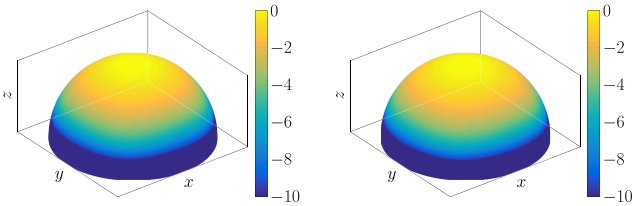

FIGURE 7. (a) bitstream coverage for two bitstreams of two orthogonal half-wave dipoles oriented along the *x*- and *y*-axes, respectively, for circularly polarized incident waves using ZF, and (b) the estimated bitstream coverage.

The bitstream coverage for the 2-bitstream case of the two orthogonal half-wave dipoles described above, is shown in Fig. 7(a) for circularly polarized incident waves by using the ZF algorithm. Comparing this figure with Fig. 1 clearly shows the effect of polarization non-orthogonality and amplitude imbalance on the MIMO efficiency, because the MIMO efficiency decreases in the presence of any of these two deficiencies. Fig. 7(b), shows the product of the two analytical MIMO efficiencies described in (6) and (7) over all angles of arrival. We observe in this figure that by using these formulas the bitstream coverage can be estimated with very good accuracy for ZF with circular polarization or SVD with inverse power allocation regardless of polarization.

Investigation of the bitstream coverage of different algorithms shows that again the different algorithm fall in the same two groups as described above. The bitstream coverage of the ZF algorithm with linear and circular polarizations is

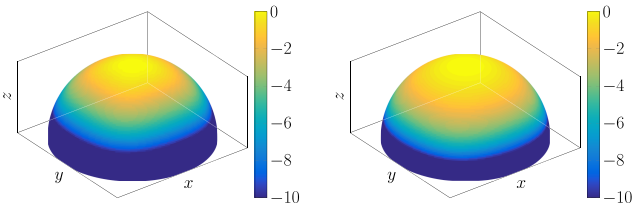

FIGURE 8. Bitstream coverage for two bitstreams of two orthogonal half-wave dipoles oriented along the *x*- and *y*-axes, respectively, ZF algorithm with (a) linear polarization, and (b) circular polarization at the transmitter side. SVD with inverse power allocation has the same shape as in (b) for both linearly and circularly polarized incident waves.

plotted in Fig. 8. The coverage of SVD algorithms are not plotted separately to avoid repetition. As we can see in Fig. 8, the coverage area of ZF with circular polarization is slightly larger than that of ZF with linear polarization.

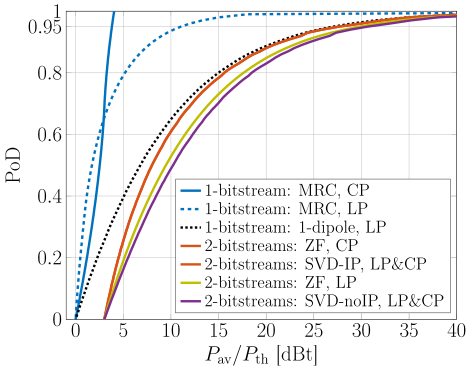

FIGURE 9. PoD curves of 1-bitstream and 2-bitstream systems for different algorithms with linear and circular polarizations. CP and LP refer to circular or linear polarization of the incident wave, respectively. IP refers to Inverse Power allocation in the SVD algorithm.

The PoD curves for random AoA and polarization for a full coverage over the whole 3D sphere are plotted in Fig. 9, i.e., the 3D Random-LOS case. We observe that in Random-LOS, for 1-bitstream systems with polarization MIMO, using a circular polarization has significant advantage over a linear polarization. For 2-bitstream systems, if the SVD algorithm is used, the choice of polarization has no effect on the system performance. Whereas if the ZF algorithm is used, again using circular polarization can improve the performance of the system. However, this improvement is not as significant as in the 1-bitstream systems. It may be noted that the ZF curve for linear polarization is not the same as the SVD curves with equal power allocation, whereas it was observed earlier that the efficiency curves are the same. This can be explained by the fact that the MIMO efficiency is calculated at the 95% PoD level where the two algorithms have almost equal performance for any AoA. But at lower levels of PoD, the two algorithms start to deviate from each other. The values in dBt (i.e., dB relative to the isotropic threshold) of different curves in Fig. 9 at 90% and 95% PoD levels are summarized in Table 1 for further reference. It should also be noted that the PoD curve is a normalized throughput. So, at the same PoD

TABLE 1. Summary of the power needed to get 90% and 95% PoD levels of the different curves in Fig. 9, i.e., for two orthogonal dipoles and the 3D random-LOS case.

bitstreams	Description	dBt @ 90% PoD	dBt @ 95% PoD
1	MRC, CP	3.6	3.8
1	MRC, LP	8.1	11.1
1	1 dipole, LP	21.1	27.1
2	ZF, CP	21.6	27.7
2	SVD-IP, LP&CP	21.6	27.7
2	ZF, LP	23.7	29.8
2	SVD-noIP, LP&CP	24.6	30.7

level, a 2-bitstream system has double the actual throughput of the 1-bitstream system.

VII. CONCLUSION

We have investigated the effects of polarization non-orthogonality and amplitude imbalance between two co-located orthogonal linearly polarized antenna ports, on the performance of 2×1 1-bitstream (SIMO case) and 2×2 2-bitstream (MIMO case) systems in Random-LOS. The former makes use of the MRC algorithm and the latter makes use of the ZF and SVD algorithms. The performance is determined in terms of MIMO efficiency, i.e., degradation of the PoDs at the 95% level. We have shown that MIMO systems in Random-LOS are not more sensitive to imbalances for two-bitstreams (MIMO) than for 1-bitstream (SIMO). There is an exception for the special case of circular polarized antennas on one side of the link and linearly polarized on the other. Then, the 1-bitstream case is not sensitive to any deficiencies, whereas the 2-bitstream case is just slightly less sensitive than the linearly-polarized transmitting case. Furthermore, we have presented two analytical formulas by which the MIMO efficiency is easily determined. It is important to be aware that orthogonally polarized antennas can have large polarization deficiencies away from boresight, even if there is no mutual coupling between the two ports. A good example is two orthogonal dipoles. This is clearly seen from the provided plots of the polarization non-orthogonality and imbalance, and the bitstream coverage plots.

REFERENCES

[1] R. W. Kreutel, D. F. DiFonzo, W. J. English, and R. W. Gruner, "Antenna technology for frequency reuse satellite communications," *Proc. IEEE*, vol. 65, no. 3, pp. 370–378, Mar. 1977.
[2] P. H. Lehne, K. Mahmood, A. A. Glazunov, P. Grønsund, and P.-S. Kildal, "Measuring user-induced randomness to evaluate smart phone performance in real environments," in *Proc. 9th Eur. Conf. Antennas Propag. (EuCAP)*, Lisbon, Portugal, Apr. 2015, pp. 1–5.
[3] M. A. Jensen and J. W. Wallace, "A review of antennas and propagation for MIMO wireless communications," *IEEE Trans. Antennas Propag.*, vol. 52, no. 11, pp. 2810–2824, Nov. 2004.
[4] T. Ingason and H. Liu, "Line-of-sight MIMO for microwave links—Adaptive dual polarized and spatially separated systems," M.S. thesis, Dept. Signals Syst., Chalmers Univ. Technol., Gothenburg, Sweden, 2009.
[5] A. A. Glazunov, V.-M. Kolmonen, and T. Laitinen, "MIMO over-the-air testing," in *LTE-Advanced and Next Generation Wireless Networks: Channel Modelling and Propagation*. Chichester, U.K.: Wiley, 2012, pp. 411–441.
[6] P. S. Kildal, C. Orlenius, and J. Carlsson, "OTA testing in multipath of antennas and wireless devices with MIMO and OFDM," *Proc. IEEE*, vol. 100, no. 7, pp. 2145–2157, Jul. 2012.
[7] A. A. Glazunov, P.-S. Kildal, J. Carlsson, M. S. Kildal, and S. Mansouri, "Impact of the spatial user distribution on the coverage antenna pattern of maximum ratio combining in random line-of-sight," in *Proc. 9th Eur. Conf. Antennas Propag. (EuCAP)*, Lisbon, Portugal, Apr. 2015, pp. 1–5.
[8] P.-S. Kildal and J. Carlsson, "New approach to OTA testing: RIMP and pure-LOS reference environments & a hypothesis," in *Proc. 7th Eur. Conf. Antennas Propag. (EuCAP)*, Gothenburg, Sweden, Apr. 2013, pp. 315–318.
[9] P.-S. Kildal, "Rethinking the wireless channel for OTA testing and network optimization by including user statistics: RIMP, pure-LOS, throughput and detection probability," in *Proc. Int. Symp. Antennas Propag. (ISAP)*, Nanjing, China, Oct. 2013, pp. 1–4.
[10] D. Cox, "Antenna diversity performance in mitigating the effects of portable radiotelephone orientation and multipath propagation," *IEEE Trans. Commun.*, vol. 31, no. 5, pp. 620–628, May 1983.
[11] S. A. Bergmann and H. W. Arnold, "Polarisation diversity in portable communications environment," *Electron. Lett.*, vol. 22, no. 11, pp. 609–610, May 1986.
[12] U. Carlberg, J. Carlsson, A. Hussain, and P.-S. Kildal, "Ray based multipath simulation tool for studying convergence and estimating ergodic capacity and diversity gain for antennas with given far-field functions," in *Proc. 20th Int. Conf. Appl. Electromagn. Commun. (ICECom)*, Dubrovnik, Croatia, Sep. 2010, pp. 1–4.
[13] P.-S. Kildal. (2015). Foundations of antennas: A unified approach for line-of-sight and multipath. Kildal Antenn AB. [Online]. Available: http://www.kildal.se
[14] P.-S. Kildal *et al.*, "Threshold receiver model for throughput of wireless devices with MIMO and frequency diversity measured in reverberation chamber," *IEEE Antennas Wireless Propag. Lett.*, vol. 10, pp. 1201–1204, 2011.
[15] A. Hussain, P. S. Kildal, and A. A. Glazunov, "Interpreting the total isotropic sensitivity and diversity gain of LTE-enabled wireless devices from over-the-air throughput measurements in reverberation chambers," *IEEE Access*, vol. 3, pp. 131–145, 2015.
[16] X. Chen, "Throughput modeling and measurement in an isotropic-scattering reverberation chamber," *IEEE Trans. Antennas Propag.*, vol. 62, no. 4, pp. 2130–2139, Apr. 2014.
[17] S. M. Moghaddam, A. A. Glazunov, J. Yang, M. Gustafsson, and P.-S. Kildal, "Comparison of 2-bitstream polarization-MIMO performance of 2 and 4-port bowtie antennas for LTE in random-LOS," in *Proc. Int. Symp. Antennas Propag. (ISAP)*, Hobart, TAS, Australia, Nov. 2015, pp. 1–4.
[18] P.-S. Kildal, K. Rosengren, J. Byun, and J. Lee, "Definition of effective diversity gain and how to measure it in a reverberation chamber," *Microw. Opt. Technol. Lett.*, vol. 34, no. 1, pp. 56–59, 2002.
[19] N. Jamaly, P.-S. Kildal, and J. Carlsson, "Compact formulas for diversity gain of two-port antennas," *IEEE Antennas Wireless Propag. Lett.*, vol. 9, pp. 970–973, 2010.
[20] X. Chen, P.-S. Kildal, and M. Gustafsson, "Characterization of implemented algorithm for MIMO spatial multiplexing in reverberation chamber," *IEEE Trans. Antennas Propag.*, vol. 61, no. 8, pp. 4400–4404, Aug. 2013.
[21] X. Chen, B. P. Einarsson, and P.-S. Kildal, "Improved MIMO throughput with inverse power allocation—Study using USRP measurement in reverberation chamber," *IEEE Antennas Wireless Propag. Lett.*, vol. 13, pp. 1494–1496, 2014.

AIDIN RAZAVI received the B.Sc. degree in electrical engineering from K. N. Toosi University of Technology, Tehran, Iran, in 2005, the M.Sc. degree in microwave engineering from Tarbiat Modares University, Tehran, in 2007, and the Swedish Licentiate and Ph.D. degrees from the Chalmers University of Technology, Gothenberg, Sweden, in 2014 and 2016, respectively. From 2007 to 2009, he was with Hamrah Telecom Company, Iran, as a Senior Engineer. From 2009 to 2011, he was with Huawei Technologies Company, as a Radio Network Planning and Optimization Engineer. His research interests include random line-of-sight propagation, OTA measurements, MIMO systems, near-field radiation, and optimal antenna apertures.

ANDRÉS ALAYÓN GLAZUNOV (SM'11) was born in Havana, Cuba, in 1969. He received the M.Sc. (Engineer-Researcher) degree in physical engineering from Peter the Great St. Petersburg Polytechnic University, Russia, in 1994, and the Ph.D. degree in electrical engineering from Lund University, Sweden, in 2009. In 2001, he was with Telia Research, Sweden, as a Senior Research Engineer. In 2003, he was a Senior Specialist of Antenna Systems and Propagation with TeliaSonera, Sweden, where he pursued research in smart antennas and MIMO, network optimization and over-the-air (OTA) performance evaluation of handsets and their impact on wireless network performance. From 2001 to 2005, he was the Swedish Delegate to the European Cost Action 273 and was active in the Handset Antenna Working Group. He has been one of the pioneers in establishing OTA measurement techniques. He has contributed to the Everest and Newcom European research projects, and to the 3GPP and the ITU standardization bodies. From 2010 to 2014, he holds a post-doctoral position with Electromagnetic Engineering Laboratory, KTH-Royal Institute of Technology, Stockholm, Sweden. He is currently an Assistant Professor with the Division of Antenna Systems, Department of Signals and Systems, Chalmers University of Technology, Gothenburg, Sweden. He is the author of various scientific and technical publications. He is the co-author and co-editor of the book titled*LTE-Advanced and Next Generation Wireless Networks* (Wiley, 2012). His current research interests include, but are not limited to, statistical signal processing, electromagnetic theory, fundamental limitations on antenna-channel interactions, RF propagation channel measurements, modelling and simulations for network optimization, and OTA testing of wireless devices.

Dr. Glazunov was a member of the Research Staff with Ericsson Research, Ericsson AB, Kista, Sweden, from 1996 to 2001, where he conducted research in the areas of advanced receiver performance evaluation for UMTS, applied electromagnetic wave propagation, and stochastic channel modelling for wireless communications systems. During this period he also contributed to the European COST Action 259 project in the directional channel modelling working group. From 2009 to 2010, he held a Marie Curie Senior Research Fellowship at the Centre for Wireless Network Design, University of Bedfordshire, U.K.

PER-SIMON KILDAL (M'82–SM'84–F'95) has been a Professor with the Chalmers University of Technology, Gothenburg, Sweden, since 1989.

He has authored an antenna textbook, and over 150 journal articles and letters, most of them in the IEEE or IET journals. He designed two very large antennas, including the Gregorian dual-reflector feed of the Arecibo radio telescope. He was the inventor of several reflector antenna feeds, the latest being the so-called Eleven Antenna.

He received two best paper awards for the articles published in the IEEE Transactions on Antennas and Propagation, and he was a recipient of the 2011 Distinguished Achievements Award from the IEEE Antennas and Propagation Society.

He pioneered the reverberation chamber into an accurate measurement tool for antennas and wireless terminals subject to Rayleigh fading. This has been successfully commercialized in Bluetest AB.

He was the originator of the concept of soft and hard surfaces, recently resulting in the gap waveguide, a new low-loss metamaterial-based transmission line advantageous in particular over 30 GHz. He received large individual grants from the Swedish research council VR and from the European Research Council ERC for research on gap waveguides.

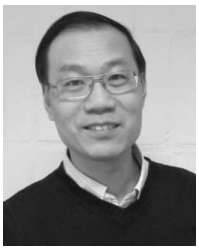

JIAN YANG (M'02–SM'10) received the B.S. degree in electrical engineering from the Nanjing University of Science and Technology, Nanjing, China, in 1982, the M.S. degree in electrical engineering from the Nanjing Research Center of Electronic Engineering, Nanjing, in 1985, and the Swedish Licentiate and Ph.D. degrees from the Chalmers University of Technology, Gothenberg, Sweden, in 1998 and 2001, respectively.

From 1985 to 1996, he was with the Nanjing Research Institute of Electronics Technology, Nanjing, as a Senior Engineer. From 1999 to 2005, he was with the Department of Electromagnetics, Chalmers University of Technology, as a Research Engineer. From 2005 to 2006, he was with Comhat AB, as a Senior Engineer. From 2006 to 2010, he was an Assistant Professor, and since 2010, he has been an Associate Professor, with the Department of Signals and Systems, Chalmers University of Technology. His research interests include 60-140 GHz antennas, THz antennas, ultra-wideband antennas and UWB feeds for reflector antennas, UWB radar systems, UWB antennas in near-field sensing applications, hat-fed antennas, reflector antennas, random design, and computational electromagnetics.